entropy

Article

Interaction between an Impurity and Nonlinear Excitations in a Polariton Condensate

Chunyu Jia and Zhaoxin Liang *

Department of Physics, Zhejiang Normal University, Jinhua 321004, China
* Correspondence: zhxliang@zjnu.edu.cn

Abstract: Exploring the dynamics of a mobile impurity immersed in field excitations is challenging, as it requires to account for the entanglement between the impurity and the surrounding excitations. To this end, the impurity's effective mass has to be considered as finite, rather than infinite. Here, we theoretically investigate the interaction between a finite-mass impurity and a dissipative soliton representing nonlinear excitations in the polariton Bose–Einstein condensate (BEC). Using the Lagrange variational method and the open-dissipative Gross–Pitaevskii equation, we analytically derive the interaction phase diagram between the impurity and a dissipative bright soliton in the polariton BEC. Depending on the impurity mass, we find the dissipative soliton colliding with the impurity can transmit through, get trapped, or be reflected. This work opens a new perspective in understanding the impurity dynamics when immersed in field excitations, as well as potential applications in information processing with polariton solitons.

Keywords: polariton condensate; soliton; entanglement; open-dissipative Gross–Pitaevskii equation

check for updates

Citation: Jia, C.; Liang, Z. Interaction between an Impurity and Nonlinear Excitations in a Polariton Condensate. *Entropy* **2022**, *24*, 1789. https://doi.org/10.3390/e24121789

Academic Editor: Hari Mohan Srivastava

Received: 9 November 2022
Accepted: 5 December 2022
Published: 7 December 2022

1. Introduction

The motion of an impurity through a dynamical medium of field excitations is a fundamental problem. In his seminal paper [1,2], Landau first studied an electron dressed by phonons. Since then, such impurity problem has appeared in different incarnations, such as the Kondo [3] and Cherenkov [4–6] effects, the polaron physics [7], and the Landau criterion [8–12] for the sound speed of a superfluid. At present, there are great efforts and interest in studying a mobile impurity in a quantum medium in diverse areas [13–19].

Central to understanding the dynamics of an impurity in a quantum many-body medium is to include the entanglement between the impurity and the surrounding excitations on a wide range of energy scales. To achieve this task, one needs to consider the impurity's effective mass as being finite, instead of infinite [8–12]. In addition, the excitations surrounding the impurity can be linear or nonlinear excitations. For instance, in ultracold quantum gases, the Bogoliubov modes are linear excitations, and dark (or bright) solitons are nonlinear excitations. Numerous theoretical studies [13–19] have already been carried out to study the interaction mechanism between the impurity and the excitations. These studies, however, mainly involve linear excitations and an impurity with an infinite mass [13–19] or finite effective mass [20]. Thus, it is highly desired to study the interaction mechanism between a quantum impurity with a finite effective mass and nonlinear excitations, such as the soliton, which is not only a key ingredient in the effective field theory, but also plays an important role in information processing [21]. In this largely unexplored area, we are interested in the interaction mechanism between an impurity and a moving bright soliton in the exciton–polariton Bose–Einstein condensate (BEC).

The exciton–polariton BEC has emerged as a novel platform for studying impurity-related problems. In comparison with previous systems [13–19], which mainly concerned equilibrium quantum media, the polariton condensates have fundamental novel aspects associated with their inherent nonequilibrium character and a strong nonlinearity. Firstly, because the polariton BEC is open-dissipative, the excitations of an homogeneous polariton condensate exhibit exotic properties. For instance, the linear excitations are provided by the diffusive Goldstone modes [22–25], with observable ghost branches of Bogoliubov excitations [26]. These have already triggered questions and studies on the definition of superfluidity and the characteristic observables in a nonequilibrium context, e.g., an extension of the standard Landau critical velocity has been proposed [11,12,27–31]. Novel kinds of nonlinear excitations have also been observed in recent experiments, such as oblique dark solitons and vortices [32–34], or bright spatial and temporal solitons [35]. Secondly, compared to the light-only solitons in optical setups, the excitonic component of the polariton leads to a weaker diffraction and stronger interparticle interactions, implying, respectively, a tighter localization and lower powers for nonlinear functionality. These appealing properties of polaritons can be used for quantum information processing [21] and quantum computation and simulation [36]. In particular, Ref. [37] engineered dissipative bright polariton solitons, whose picosecond response time made them more useful for ultrafast information processing than the light-only solitons of semiconductor cavity lasers. Thus, a timely question arises: In a nonequilibrium polariton BEC, what is the interaction mechanism between an impurity with a finite effective mass and a dynamical medium with nonlinear excitations?

In this work, we theoretically investigate the interaction between a finite-mass impurity and the dissipative bright soliton in a polariton BEC. By using the Lagrange variational method in the framework of the open-dissipative Gross–Pitaevskii equation, we analytically derive the interaction phase diagram. Depending on the impurity mass, we find that the dissipative soliton colliding with the impurity can have three fates, i.e., it can transmit through, get trapped, or be reflected. Our analytical analysis agrees well with numerical simulations based on the open-dissipative Gross–Pitaevskii equation.

The rest of the paper is organized as follows. In Section 2, we present the model which describes a polariton condensate. Furthermore, we derive the analytic expression of the interaction using the Lagrange variational method. Section 3 investigate the influence of the effective mass of the impurity on the interaction phase diagram between a soliton and an impurity in a polariton condensate, by means of a direct simulation of the motion equations of variational parameters and the Gross–Pitaevskii equation. Various interaction effects such as transmission, reflection, and trapping of the soliton by a repulsive impurity are described and verified by direct simulations of the equation. Finally, Section 4 provides a summary and conclusions for this research.

2. The Theoretical Model and Lagrangian Approach

We consider an exciton–polariton BEC under nonresonant pumping, which is created in a wire-shaped microcavity [38] that bounds the polaritons to a quasi-one-dimensional (1D) channel. In the mean field theory, the time evolution of the polariton field is governed by an effectively 1D driven-dissipative GPE for the condensate order parameter $\psi(x,t)$, which is coupled to a rate equation for the density $n_R(x,t)$ of reservoir polaritons [25,39–42], i.e.,

$$\begin{aligned} i\hbar\frac{\partial\psi}{\partial t} &= \Big[-\frac{\hbar^2}{2m}\frac{\partial^2}{\partial x^2}+V_{\mathrm{imp}}+g_C|\psi|^2+g_R n_R \\ &+ \frac{i\hbar}{2}(Rn_R-\gamma_C)\Big]\psi+P_{\mathrm{ad}}(x)\psi, \end{aligned} \tag{1}$$

$$\frac{\partial n_R}{\partial t} = P_{\mathrm{incoh}}(x)-\Big(\gamma_R+R|\psi|^2\Big)n_R. \tag{2}$$

In Equations (1) and (2), the m is the effective mass of lower polaritons, P is the off-resonant continuous-wave pumping rate, γ_C and γ_R denote the lifetimes of the condensate and reservoir polaritons, respectively, R is the stimulated scattering rate of reservoir polaritons into the condensate, g_C characterizes the strengths of the polariton interaction, while g_R denotes the interaction strength between the reservoir and the polaritons. The impurity potential [39,43] is $V_{\rm imp} = -V_0\delta(x)$, with the strength V_0. The $P_{\rm ad}(x)$ in Equation (1) and $P_{\rm incoh}(x)$ in Equation (2) are the incoherent pumping rates on the condensate and reservoir [44], respectively. The parameters g_C, g_R, and R have been rescaled into the one-dimensional case by the width d of the nanowire thickness, i.e., $g_C \to g_C/\sqrt{2\pi d}$, $g_R \to g_R/\sqrt{2\pi d}$, $R \to R/\sqrt{2\pi d}$. We aim to investigate the interaction mechanism between the impurity and the nonlinear excitations.

As the first step, let us determine the steady state of Equations (1) and (2), which will provide the density background for the nonlinear excitations. Following Ref. [40], when the pumping rate P in Equation (2) exceeds the critical value $P_{\rm th} = \gamma_R\gamma_C/R$, a stable condensate with the condensate density $n_C^0 = (P_{\rm incoh} - P_{\rm th})/\gamma_C$ can be created. The corresponding steady-state reservoir density is $n_R^0 = \gamma_C/R$, with $P_{\rm incoh} = P_{\rm stat}$.

By rescaling $\psi \to \psi/\sqrt{n_C^0}$ and denoting $m_R = n_R - n_R^0$, Equations (1) and (2) can be recast into a dimensionless form as

$$\begin{aligned} i\frac{\partial\psi}{\partial t} &+ \frac{1}{2}\frac{\partial^2\psi}{\partial x^2} + |\psi|^2\psi + \gamma\delta(x)\psi = 2|\psi|^2\psi + \bar{P}_{\rm ad}(x)\psi \\ &+ (\bar{g}_R m_R + \frac{i}{2}\bar{R} m_R)\psi, \end{aligned} \tag{3}$$

$$\frac{\partial m_R}{\partial t} = \bar{P}_{\rm incoh}(x) + \bar{\gamma}_C(1-|\psi|^2) - \bar{\gamma}_R m_R - \bar{R}|\psi|^2 m_R. \tag{4}$$

where $\bar{g}_R = g_R/g_C$, $\bar{\gamma}_C = \gamma_C\bar{\gamma}_R/\gamma_R$, $\bar{P}_{\rm ad}(x) = P_{\rm ad}/g_C n_C^0$,$\bar{P}_{\rm incoh} = (P_{\rm incoh}(x) - P_{\rm stat})/g_C n_C^0$ and $\bar{R} = \hbar R/g_C n_C^0$. The term with $\gamma = V_0/g_C n_C^0$ describes the impurity potential. Moreover, we have measured the time t and the space coordinate x in the units of $\tau = \hbar g n_C^0$ and $\xi = \sqrt{\hbar^2/mgn_C^0}$. Equations (3) and (4) are the starting point for our subsequent investigation of the interaction between the impurity and the nonlinear excitations in the polariton BEC. Note that the nonequilibrium nature of the model system is captured by the parameters of $\bar{R}$ in Equation (3).

We are interested in the fast reservoir limit, where the reservoir density in Equation (4) can be written as [40]

$$m_R = \frac{\bar{P}_{\rm incoh}(x)}{\bar{\gamma}_R} + \frac{\bar{\gamma}_C}{\bar{\gamma}_R}(1 - |\psi|^2). \tag{5}$$

where $\bar{P}_{\rm incoh}(x) = \bar{P}^c_{\rm incoh} + \bar{P}^v_{\rm incoh}(x)$, with the constant pumping rate $\bar{P}^c_{\rm incoh}$ and the spatially dependent pumping rate $\bar{P}^v_{\rm incoh}(x)$. Following Ref. [40], we insert Equation (5) into Equation (3), and rewrite Equation (3) as

$$\begin{aligned} i\frac{\partial\psi}{\partial t} + \frac{1}{2}\frac{\partial^2\psi}{\partial x^2} &+ |\psi|^2\psi \\ &+ \gamma\delta(x)\psi = \frac{i}{2}[P(x) - \sigma - \chi|\psi|^2]\psi. \end{aligned} \tag{6}$$

Here, we model $P(x) = \bar{R}\bar{P}^v_{\rm incoh}(x)/\bar{\gamma}_R$ as a spatially modulated Gaussian function with the power P_0 and width ω, i.e., $P(x) = P_0 e^{-x^2/\omega^2}$; the parameters $\sigma = -(\bar{P}^c_{\rm incoh} + \bar{\gamma}_C)\bar{R}/\bar{\gamma}_R$ and $\chi = \bar{R}\bar{\gamma}_C/\bar{\gamma}_R$ are referred to as the polariton loss rate and the gain saturation, respectively. In deriving Equation (6), the incoherent pumping of $\bar{P}_{\rm ad}(x)$ is adjusted to be $\bar{P}_{\rm coh}(x) = -2|\psi|^2 - \bar{g}_R m_R$ within the current experimental capability [44–46]. Below, we investigate the interaction between a bright soliton and the impurity as captured by the γ term in Equation (6).

Equation (6) can be viewed as a nonlinear Schrödinger equation subjected to a time-dependent perturbation of the form $D(\psi) = i[P(x) - \sigma - \chi|\psi|^2]\psi/2$. As a benchmark, let us recapitulate the unperturbed case $D(\psi) = 0$ without the open-dissipative effects: (i) for a vanishing nonlinearity in Equation (6), Equation (6) can be simplified into the linear Schrödinger equation with the delta-potential. It has the well-known exact solution $\psi_{\rm im}(x) = \sqrt{\lambda}e^{-\lambda|x|}$ with $\lambda = \gamma$ that describes the impurity; (ii) for a vanishing delta-potential $\gamma \rightarrow 0$, Equation (6) allows for the exact soliton solution $\psi_{\rm so} = {\rm sech}(\eta(x-ct))\exp(i(\eta^2-c^2)t/2+icx)$ with an arbitrary amplitude η.

Next, we take into account the open-dissipative effects captured by $D(\psi) = i[P(x) - \sigma - \chi|\psi|^2]\psi/2$ in Equation (6). Since $\psi_{\rm im}(x)$ and $\psi_{\rm so}$ are no longer the exact solutions of Equation (6), we exploit the Lagrangian approach of the perturbation theory to treat the open-dissipative effects. We assume a trial wave function as a combination of the bright soliton and impurity mode

$$\begin{aligned} \psi(x,t) &= \Big[\eta(t){\rm sech}[\eta(t)(x-z(t))]e^{i\kappa(t)x} \\ &+ a(t)\sqrt{\lambda(t)}e^{-\lambda(t)|x|+i\varphi(t)}\Big]e^{i\phi(t)}, \end{aligned} \tag{7}$$

where η, z, ϕ, κ, a, λ, and φ are the variational parameters. Specifically, $\phi(t)$ is the global phase of the trial wave function, $\eta(t)$ and $Z(t)$ are the amplitudes and center position of the bright soliton, respectively, $\kappa(t)$ is referred to as the wavenumber of the soliton, $a(t)$ and $\lambda(t)$ are associated with the strength of the variable function induced by the impurity, and $\varphi(t)$ is the relative phase between the soliton and impurity-induced function.

The key assumption underlying the ansatz (7) is that the functional forms of the soliton and the impurity-induced function are preserved in the presence of perturbation, whereas the corresponding parameters become slowly time-dependent. The time evolution of the parameters in Equation (7) can be obtained via the Euler-Lagrangian equations for the dissipative system [47–51]

$$\frac{\partial L}{\partial q_i} - \frac{d}{dt}\left(\frac{\partial L}{\partial \dot{q}_i}\right) = 2\mathcal{R}\left(\int_{-\infty}^{+\infty} D^*(\psi)\frac{\partial \psi}{\partial q_i}\right), \tag{8}$$

with $\dot{q}_i \equiv dq_i/dt$ and $q_i = \eta, z, \phi, \kappa, a, \lambda, \varphi$, and $\mathcal{R}$ labels the real part of the expression. In Equation (8), the Lagrangian $L = \int_{-\infty}^{+\infty} \mathcal{L}dx$ is referred to as the average Lagrangian of Equation (6) with $D(\psi) = 0$, where the Lagrangian density $\mathcal{L}$ is given by

$$\mathcal{L} = \frac{i}{2}(\psi^*\psi_t - \psi\psi_t^*) - \frac{1}{2}|\psi_x|^2 + \frac{1}{2}|\psi|^4 + \gamma|\psi|^2\delta(x). \tag{9}$$

Inserting the ansatz (7) into Equation (9), we calculate the average Lagrangian L in Equation (8) as

$$\begin{aligned} L &= -2\eta\dot{\phi} - 2\dot{\kappa}z - a^2(\dot{\phi}+\dot{\varphi}) + \frac{\eta^3}{3} - \kappa^2\eta - \frac{a^2\lambda^2}{2} + \gamma a^2\lambda \\ &+ \gamma\eta^2{\rm sech}(z)^2 + 2\gamma\eta a\sqrt{\lambda}{\rm sech}(z)\cos(\varphi) + O\left(a^4\right). \end{aligned} \tag{10}$$

Here, we have ignored the higher-order terms of $O(a^4)$, as inspired by Ref. [52]. Physically, this corresponds to ignoring the direct interaction between the soliton and the local mode, except for the energy exchange through the defect. This approximation will be justified a posteriori by comparing the analytical results from Equation (10) and the simulation results based on Equation (6).

By substituting Equation (10) into Equation (8), we obtain the equations of motion for the variational parameters ϕ, κ, φ, z, a, η, and λ in Equation (8) as

$$\dot{\eta} = \frac{1}{12}\left[(6a^2 + 12\eta)(P_0 - \sigma) - 12a\dot{a} - 8\chi\eta^3 - 3\chi a^4\lambda\right], \tag{11a}$$

$$\dot{z} = \frac{1}{3}\left[3z(P_0 - \sigma) - 2\chi z\eta^2 + 3\eta\kappa\right], \tag{11b}$$

$$\dot{a} = \frac{1}{4}\left[2a(P_0 - \sigma) + 4\gamma\mathrm{sech}[z]\sin[\varphi]\eta\sqrt{\lambda} - \chi a^3\lambda\right], \tag{11c}$$

$$\dot{\kappa} = -\gamma\mathrm{sech}[z]^2\tanh[z]\eta^2 - \gamma a\cos[z]\mathrm{sech}[z]\tanh[z]\eta\sqrt{\lambda}, \tag{11d}$$

$$\dot{\varphi} = -\gamma\mathrm{sech}[z]^2\eta - \frac{\eta^2}{2} + \frac{\kappa^2}{2} - \gamma a\cos[\varphi]\mathrm{sech}[z]\sqrt{\lambda} + \gamma a^{-1}\cos[\varphi]\mathrm{sech}[z]\eta\sqrt{\lambda} + \gamma\lambda - \frac{\lambda^2}{2}, \tag{11e}$$

$$\dot{\phi} = \gamma\mathrm{sech}[z]^2\eta + \frac{\eta^2 - \kappa^2}{2} + \gamma a\cos[\varphi]\mathrm{sech}[z]\sqrt{\lambda}, \tag{11f}$$

$$0 = a(\gamma - \lambda) + \gamma\eta\lambda^{-1/2}\cos[\varphi]\mathrm{sech}[z]. \tag{11g}$$

Equations (11a)–(11g) are the key results of this work, which describe the interaction of an impurity and a bright soliton in the polariton condensate. Note that without the dissipation (i.e., $P_0 = \sigma = \chi = 0$), the above equations obviously reproduce the result of Ref. [52]. According to Equations (11a)–(11c), the nonequilibrium nature of the polariton condensates will directly affect the soliton's center position z and its amplitude η, as well as the impurity's amplitude $a[t]\lambda[t]^{1/2}$. Since ϕ does not appear in Equations (11a) and (11b), the relevant equations for our study, Equation (11f) for $\dot{\phi}$ is not important. Equation (11c), on the other hand, is crucial because it shows that the moving soliton excites the local mode. Note that Equation (11g) without the soliton ($\eta = 0$) gives the correct value $\lambda = \gamma$ for the spatial decay of the impurity mode.

3. Interaction between an Impurity and a Bright Soliton

In the previous section, we used the Lagrangian approach to analytically derive Equations (11a)–(11g). Below, we construct the interaction phase diagram by solving Equations (11a)–(11g) and comparing the results with the exact numerical simulations of the dynamics governed by Equation (6), supplemented with the initial function of Equation (11b).

Let us first specify the initial conditions of Equations (11a)–(11g). We assume the soliton is initially at $z = -10$, far from the impurity at $z = 0$. The initial amplitude and velocity of the soliton are chosen as $\eta = 0.1$ and $\kappa = 0.02$, respectively. For other parameters (a, λ, φ and ϕ), we set their initial values as 0.

We then solve the time-evolutions of the parameters z, a, κ, and φ from Equations (11b)–(11e). The soliton amplitude η is determined by Equations (11a)–(11c), and λ is calculated from Equation (11g). In addition, Equation (11g) allows us to follow independently the evolution of the soliton and the impurity. The solutions to Equations (11a)–(11g) are plotted in the left column of Figures 1–3. To validate our variational approach, we also show the numerical results from the direct solutions of Equation (6) on the right column of Figures 1–3.

In understanding the interaction between the impurity and the quantum many-body medium, we emphasize the key role of the effective mass of the impurity [5,6]. For an infinite mass, corresponding to a pinned impurity [5,53], a kinematic scale is set up by the sound speed of the superfluid according to the Landau criterion. In contrast, an impurity with a finite mass is expected to recoil due to the interactions with the surrounding quantum gas, yielding novel physics beyond the kinematic picture [6]. Indeed, quantum fluctuations already become highly relevant to the dynamics for the slowly moving impurities with a finite mass.

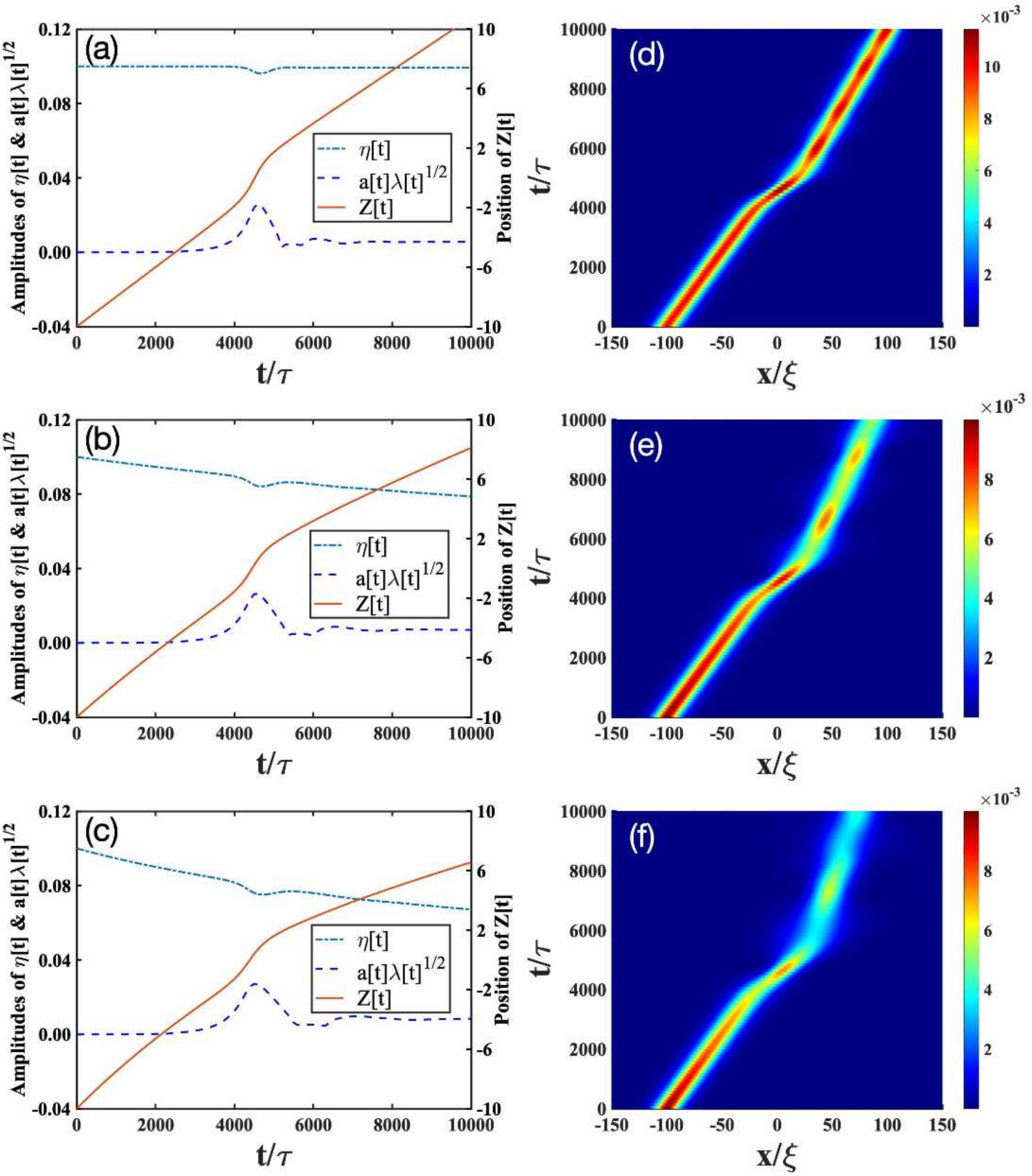

Figure 1. Transmission scenario corresponding to the bright soliton with the initial value $\eta = 0.01$ passing through the impurity with a strength of $\gamma = 0.02$. The analytical results of Equations (11a)–(11g) and the numerical simulation based on Equation (6) are plotted in the left and right columns, respectively. In (**a**–**c**), the positions Z of the bright soliton are plotted by solid lines and scaled on the right axis; the amplitudes η of the bright soliton are plotted by dash-dotted lines and scaled on the left axis; the impurity amplitudes of $a\lambda^{1/2}$ are plotted by the dashed lines and scaled on the left axis. The other parameters are given as follows: $P_0 = \sigma = \chi = 0$ in (**a**,**d**); $P_0 = \sigma = \chi = 0.005$ in (**b**,**e**); $P_0 = \sigma = \chi = 0.01$ in (**c**,**f**).

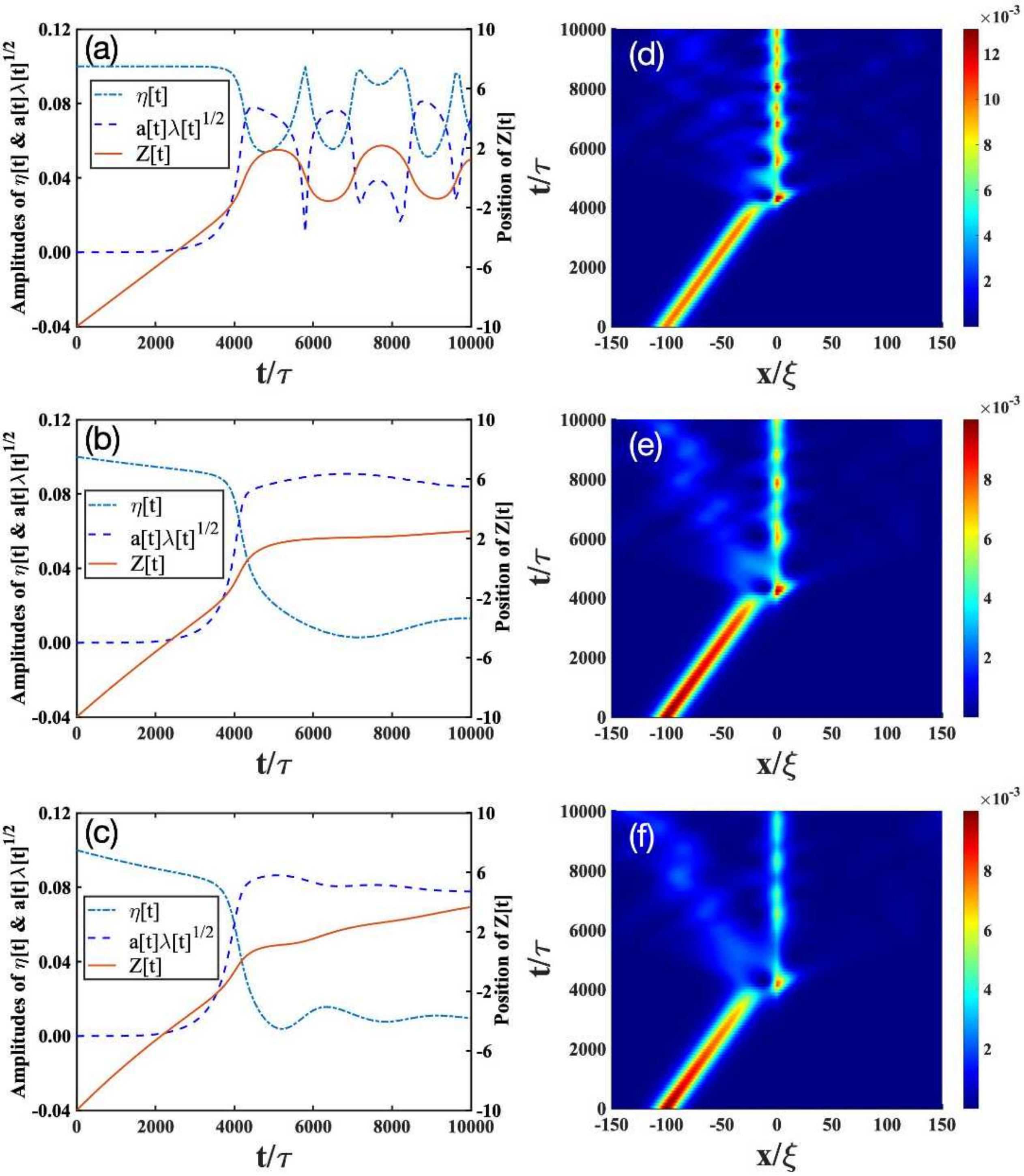

Figure 2. Trapping scenario corresponding to the bright soliton with the initial value $\eta = 0.01$ passing through the impurity with a strength of $\gamma = 0.05$. The other parameters and descriptions about the figures are the same as the ones in Figure 1.

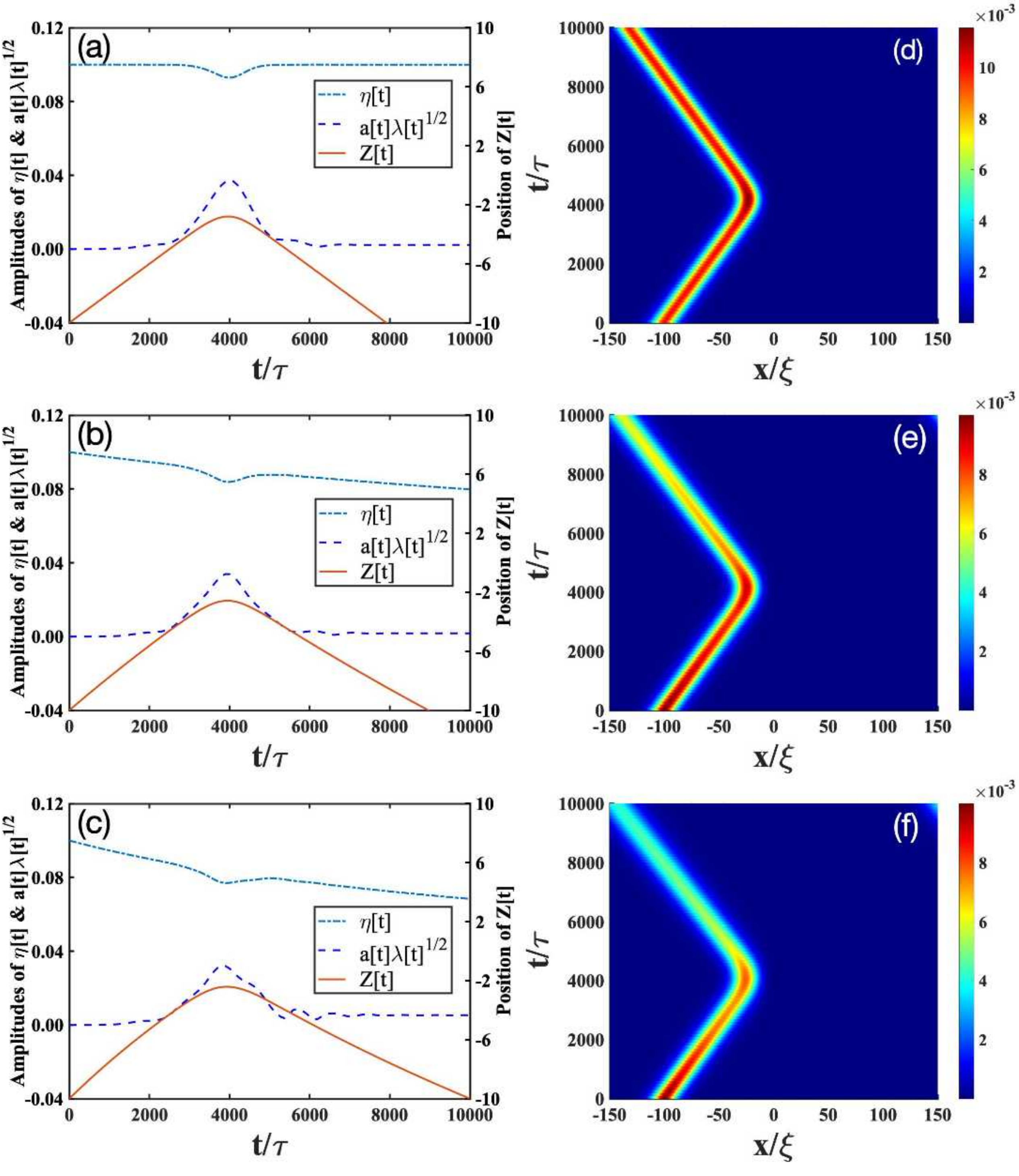

Figure 3. Reflection scenario corresponding to the bright soliton with the initial value $\eta = 0.01$ passing through the impurity with a strength of $\gamma = 0.14$. The other parameters and descriptions about the figures are the same as the ones in Figure 1.

Figures 1–3 show the interaction diagrams between the impurity and a bright soliton under various impurity trap strengths γ. Different γ's correspond to different effective masses m_{eff} of the impurity [52]. For $\gamma = 0.02, 0.05, 0.14$ used in the plots, we have $m_{\text{eff}} = 1.04, 1.10, 1.28$. In the following, we analyze how the impurity–soliton interaction is affected by the open-dissipative nature of the condensate, as captured by the parameters of P_0, σ, and χ in Equation (6).

The results for $P_0 = \sigma = \chi = 0$ in the absence of dissipation [52] are plotted in Figures 1a–3a, respectively. Depending on γ, we find there exist three scenarios. (i) The transmission scenario (Figure 1a): when γ is small, the bright soliton directly transmits through the impurity. (ii) The trapping reflection scenario (Figure 2a): when γ increases, the bright soliton can be trapped by the impurity (see Figure 2a). (iii) The reflection scenario (Figure 3a): when γ is strong enough, the bright soliton is reflected by the impurity.

To compare the interaction of the soliton with the impurity in the presence and absence of dissipation, we change the dissipative parameters of P_0, σ, and χ in each scenario:

(i) Transmission scenario: As mentioned before, in the absence of dissipation (Figure 1a), the bright soliton can simply pass through a light impurity ($m_{\text{eff}} = 1.04$), almost unaffected by the latter. The dotted lines in Figure 1a denotes the amplitude of the impurity. There, the appearance of the maximal amplitude of the impurity indicates that the impurity mode can be excited during the collision with the bright soliton, but after the collision, the excitation returns to a very small level. This analysis is consistent with Figure 1d obtained from the numerical simulation of Equation (6). Thus, we conclude that the analytical results in Equations (11a)–(11g) not only provide a good solution to Equation (6), but also allow us to follow independently the evolution of the bright soliton and the impurity. In the presence of dissipation, the amplitude of soliton gradually decreases after the collision with the impurity; see the solid lines in Figure 1b,c. These results are consistent with the full numerical simulations in Figure 1e,f. Comparing Figure 1b,c, therefore, we see that the soliton amplitude decays faster when the dissipation parameter increases.

(ii) Trapping scenario: In the absence of dissipation (Figure 2a,d), the bright soliton can be trapped by an impurity with a moderate mass ($m_{\text{eff}} = 1.10$), as indicated by the position of the bright soliton (solid lines in Figure 2a). Furthermore, the impurity mode (dashed lines in Figure 2a) is strongly excited and begins to oscillate, whereas the soliton amplitude (dashed-dotted lines in Figure 2a) decreases drastically. This result is verified by the numerical simulations in Figure 2d. In the presence of dissipation (Figure 2b,c,e,f), the bright soliton can still be trapped by the impurity, but the oscillating behavior of the bright soliton begins to disappear. This can be understood, as the dissipation will destroy the low-energy excitations generated from the collisions of the bright soliton and the impurity.

(iii) Reflection scenario: In the absence of dissipation (Figure 3a,d), the bright soliton can be reflected by a heavy impurity ($m_{\text{eff}} = 1.28$). In contrast to the above transmission and trapping scenarios, dissipation has relatively small effects on the reflection scenario, as shown in Figure 3b,d–f. This can be expected, because the heavier the impurity is, the less excitations are created from the collisions.

4. Conclusions

In summary, we investigated the interaction dynamics of a soliton with an impurity mode in the exciton–polariton condensates excited by a nonresonant pump. Our study was based on the Lagrange variational approach, which allowed us to analytically derive the equations of motion for each variational parameter. Depending on the interaction strength between the soliton and the impurity, we observed the occurrence of transmission, reflection, and trapping of the soliton by the impurity. We showed that these effects were weakened with the increase of dissipation. Our analytical results of the interaction phase diagram agreed well with the numerical results of the open-dissipative Gross–Pitaevskii equation. The present work goes beyond prior research studies in the context of equilibrium systems, opening a new perspective toward understanding the nonequilibrium dynamics of a mobile impurity immersed the field excitations.

Author Contributions: Conceptualization, Z.L.; Investigation, C.J.; Methodology, C.J. and Z.L.; software, C.J.; writing—original draft preparation, C.J.; writing—review and editing, Z.L.; supervision, Z.L.; All authors have read and agreed to the published version of the manuscript.

Funding: This work was supported by the Zhejiang Provincial Natural Science Foundation (grant no. LZ21A040001), the National Natural Science Foundation of China (grant no. 12074344) and the key projects of the Natural Science Foundation of China (grant no. 11835011).

Institutional Review Board Statement: Not applicable.

Data Availability Statement: Not applicable.

Acknowledgments: We thank Yiling Zhang for stimulating discussions. This work was supported by the Zhejiang Provincial Natural Science Foundation (grant no. LZ21A040001), the National Natural Science Foundation of China (grant no. 12074344) and the key projects of the Natural Science Foundation of China (grant no. 11835011).

Conflicts of Interest: The authors declare no conflict of interest.

References

1. Landau, L.D. The Movement of Electrons in the Crystal Lattice. *Phys. Z. Sowjetunion* **1933**, *3*, 644.
2. Landau, L.D.; Pekar, S.I. Effective Mass of a Polaron. *J. Exp. Theor. Phys.* **1948**, *18*, 419.
3. Hewson, A.C. *The Kondo Problem to Heavy Fermions*; Cambridge University: Cambridge, UK, 1993.
4. Bolotovskii, B.M. Vavilov–Cherenkov radiation: Its discovery and application. *Phys.-Uspekhi* **2009**, *52*, 1099–1110. [CrossRef]
5. Carusotto, I.; Hu, S.X.; Collins, L.A.; Smerzi, A. Bogoliubov-Čerenkov Radiation in a Bose-Einstein Condensate Flowing against an Obstacle. *Phys. Rev. Lett.* **2006**, *97*, 260403. [CrossRef]
6. Seetharam, K.; Shchadilova, Y.; Grusdt, F.; Zvonarev, M.B.; Demler, E. Dynamical Quantum Cherenkov Transition of Fast Impurities in Quantum Liquids. *Phys. Rev. Lett.* **2021**, *127*, 185302. [CrossRef]
7. Mahan, G. *Many-Particle Physics*; Kluwer Academic/Plenum Publishers: New York, NY, USA, 2000.
8. Astrakharchik, G.E.; Boronat, J.; Casulleras, J.; Giorgini, S. Superfluidity versus Bose-Einstein condensation in a Bose gas with disorder. *Phys. Rev. A* **2002**, *66*, 23603. [CrossRef]
9. Wouters, M.; Carusotto, I. Superfluidity and Critical Velocities in Nonequilibrium Bose-Einstein Condensates. *Phys. Rev. Lett.* **2010**, *105*, 20602. [CrossRef]
10. Liang, Z.X.; Dong, X.; Zhang, Z.D.; Wu, B. Sound speed of a Bose-Einstein condensate in an optical lattice. *Phys. Rev. A* **2008**, *78*, 23622. [CrossRef]
11. Amelio, I.; Carusotto, I. Perspectives in superfluidity in resonantly driven polariton fluids. *Phys. Rev. B* **2020**, *101*, 64505. [CrossRef]
12. He, P.S.; Liang, Z. Drag force of an exciton-polariton condensate under nonresonant pumping. *Phys. Rev. A* **2021**, *103*, 13303. [CrossRef]
13. Chevy, F.; Mora, C. Ultra-cold polarized Fermi gases. *Rep. Prog. Phys.* **2010**, *73*, 112401. [CrossRef]
14. Massignan, P.; Zaccanti, M.; Bruun, G.M. Polarons, dressed molecules and itinerant ferromagnetism in ultracold Fermi gases. *Rep. Prog. Phys.* **2014**, *77*, 34401. [CrossRef]
15. Adlong, H.S.; Liu, W.E.; Scazza, F.; Zaccanti, M.; Oppong, N.D.; Fölling, S.; Parish, M.M.; Levinsen, J. Quasiparticle Lifetime of the Repulsive Fermi Polaron. *Phys. Rev. Lett.* **2020**, *125*, 133401. [CrossRef]
16. Schmidt, R.; Knap, M.; Ivanov, D.A.; You, J.S.; Cetina, M.; Demler, E. Universal many-body response of heavy impurities coupled to a Fermi sea: A review of recent progress. *Rep. Prog. Phys.* **2018**, *81*, 24401. [CrossRef]
17. Jørgensen, N.B.; Wacker, L.; Skalmstang, K.T.; Parish, M.M.; Levinsen, J.; Christensen, R.S.; Bruun, G.M.; Arlt, J.J. Observation of Attractive and Repulsive Polarons in a Bose-Einstein Condensate. *Phys. Rev. Lett.* **2016**, *117*, 55302. [CrossRef] [PubMed]
18. Hu, M.G.; Van de Graaff, M.J.; Kedar, D.; Corson, J.P.; Cornell, E.A.; Jin, D.S. Bose Polarons in the Strongly Interacting Regime. *Phys. Rev. Lett.* **2016**, *117*, 55301. [CrossRef] [PubMed]
19. Yan, Z.Z.; Ni, Y.; Robens, C.; Zwierlein, M.W. Bose polarons near quantum criticality. *Science* **2020**, *368*, 190–194. [CrossRef] [PubMed]
20. Vashisht, A.; Richard, M.; Minguzzi, A. Bose polaron in a quantum fluid of light. *SciPost Phys.* **2022**, *12*, 8. [CrossRef]
21. Flayac, H.; Solnyshkov, D.D.; Shelykh, I.A.; Malpuech, G. Transmutation of Skyrmions to Half-Solitons Driven by the Nonlinear Optical Spin Hall Effect. *Phys. Rev. Lett.* **2013**, *110*, 16404. [CrossRef]
22. Wouters, M.; Carusotto, I. Excitations in a Nonequilibrium Bose-Einstein Condensate of Exciton Polaritons. *Phys. Rev. Lett.* **2007**, *99*, 140402. [CrossRef]
23. Szymańska, M.H.; Keeling, J.; Littlewood, P.B. Nonequilibrium Quantum Condensation in an Incoherently Pumped Dissipative System. *Phys. Rev. Lett.* **2006**, *96*, 230602. [CrossRef]
24. Byrnes, T.; Horikiri, T.; Ishida, N.; Fraser, M.; Yamamoto, Y. Negative Bogoliubov dispersion in exciton-polariton condensates. *Phys. Rev. B* **2012**, *85*, 75130. [CrossRef]
25. Xu, X.; Hu, Y.; Zhang, Z.; Liang, Z. Spinor polariton condensates under nonresonant pumping: Steady states and elementary excitations. *Phys. Rev. B* **2017**, *96*, 144511. [CrossRef]

26. Pieczarka, M.; Syperek, M.; Dusanowski, L.; Misiewicz, J.; Langer, F.; Forchel, A.; Kamp, M.; Schneider, C.; Höfling, S.; Kavokin, A.; et al. Ghost Branch Photoluminescence From a Polariton Fluid Under Nonresonant Excitation. *Phys. Rev. Lett.* **2015**, *115*, 186401. [CrossRef] [PubMed]
27. Janot, A.; Hyart, T.; Eastham, P.R.; Rosenow, B. Superfluid Stiffness of a Driven Dissipative Condensate with Disorder. *Phys. Rev. Lett.* **2013**, *111*, 230403. [CrossRef] [PubMed]
28. Keeling, J. Superfluid Density of an Open Dissipative Condensate. *Phys. Rev. Lett.* **2011**, *107*, 080402. [CrossRef] [PubMed]
29. Van Regemortel, M.; Wouters, M. Negative drag in nonequilibrium polariton quantum fluids. *Phys. Rev. B* **2014**, *89*, 85303. [CrossRef]
30. Gladilin, V.N.; Wouters, M. Normal and superfluid fractions of inhomogeneous nonequilibrium quantum fluids. *Phys. Rev. B* **2016**, *93*, 134511. [CrossRef]
31. Juggins, R.T.; Keeling, J.; Szymańska, M.H. Coherently driven microcavity-polaritons and the question of superfluidity. *Nat. Commun.* **2018**, *9*, 4062. [CrossRef]
32. Grosso, G.; Nardin, G.; Morier-Genoud, F.; Léger, Y.; Deveaud-Plédran, B. Soliton Instabilities and Vortex Street Formation in a Polariton Quantum Fluid. *Phys. Rev. Lett.* **2011**, *107*, 245301. [CrossRef]
33. Akhmerov, A.R. Topological quantum computation away from the ground state using Majorana fermions. *Phys. Rev. B* **2010**, *82*, 20509. [CrossRef]
34. Amo, A.; Pigeon, S.; Sanvitto, D.; Sala, V.G.; Hivet, R.; Carusotto, I.; Pisanello, F.; Lemenager, G.; Houdre, R.; Giacobino, E.; et al. Polariton Superfluids Reveal Quantum Hydrodynamic Solitons. *Science* **2011**, *332*, 1167–1170. [CrossRef] [PubMed]
35. Barland, S.; Giudici, M.; Tissoni, G.; Tredicce, J.R.; Brambilla, M.; Lugiato, L.; Prati, F.; Barbay, S.; Kuszelewicz, R.; Ackemann, T.; et al. Solitons in semiconductor microcavities. *Nat. Photonics* **2012**, *6*, 204. [CrossRef]
36. Sanvitto, D.; Kéna-Cohen, S. The road towards polaritonic devices. *Nat. Mater.* **2016**, *15*, 1061–1073. [CrossRef]
37. Sich, M.; Krizhanovskii, D.N.; Skolnick, M.S.; Gorbach, A.V.; Hartley, R.; Skryabin, D.V.; Cerda-Méndez, E.A.; Biermann, K.; Hey, R.; Santos, P.V. Observation of bright polariton solitons in a semiconductor microcavity. *Nat. Photonics* **2012**, *6*, 50–55. [CrossRef]
38. Wertz, E.; Ferrier, L.; Solnyshkov, D.D.; Johne, R.; Sanvitto, D.; Lemaître, A.; Sagnes, I.; Grousson, R.; Kavokin, A.V.; Senellart, P.; et al. Spontaneous formation and optical manipulation of extended polariton condensates. *Nat. Phys.* **2010**, *6*, 860–864. [CrossRef]
39. Keeling, J.; Berloff, N.G. Spontaneous Rotating Vortex Lattices in a Pumped Decaying Condensate. *Phys. Rev. Lett.* **2008**, *100*, 250401. [CrossRef] [PubMed]
40. Smirnov, L.A.; Smirnova, D.A.; Ostrovskaya, E.A.; Kivshar, Y.S. Dynamics and stability of dark solitons in exciton-polariton condensates. *Phys. Rev. B* **2014**, *89*, 235310. [CrossRef]
41. Yu, Z.F.; Xue, J.K.; Zhuang, L.; Zhao, J.; Liu, W.M. Non-Hermitian spectrum and multistability in exciton-polariton condensates. *Phys. Rev. B* **2021**, *104*, 235408. [CrossRef]
42. Sabari, S.; Kumar, R.K.; Radha, R.; Muruganandam, P. Stability window of trapless polariton Bose-Einstein condensates. *Phys. Rev. B* **2022**, *105*, 224315. [CrossRef]
43. Cristofolini, P.; Dreismann, A.; Christmann, G.; Franchetti, G.; Berloff, N.G.; Tsotsis, P.; Hatzopoulos, Z.; Savvidis, P.G.; Baumberg, J.J. Optical Superfluid Phase Transitions and Trapping of Polariton Condensates. *Phys. Rev. Lett.* **2013**, *110*, 186403. [CrossRef] [PubMed]
44. Sitnik, K.A.; Alyatkin, S.; Töpfer, J.D.; Gnusov, I.; Cookson, T.; Sigurdsson, H.; Lagoudakis, P.G. Spontaneous Formation of Time-Periodic Vortex Cluster in Nonlinear Fluids of Light. *Phys. Rev. Lett.* **2022**, *128*, 237402. [CrossRef] [PubMed]
45. Cerna, R.; Sarchi, D.; Paraïso, T.K.; Nardin, G.; Léger, Y.; Richard, M.; Pietka, B.; El Daif, O.; Morier-Genoud, F.; Savona, V.; et al. Coherent optical control of the wave function of zero-dimensional exciton polaritons. *Phys. Rev. B* **2009**, *80*, 121309. [CrossRef]
46. Wang, Y.; Sigurdsson, H.; Töpfer, J.D.; Lagoudakis, P.G. Reservoir optics with exciton-polariton condensates. *Phys. Rev. B* **2021**, *104*, 235306. [CrossRef]
47. Kivshar, Y.S.; Królikowski, W. Lagrangian approach for dark solitons. *Opt. Commun.* **1995**, *114*, 353–362. [CrossRef]
48. Theocharis, G.; Schmelcher, P.; Oberthaler, M.K.; Kevrekidis, P.G.; Frantzeskakis, D.J. Lagrangian approach to the dynamics of dark matter-wave solitons. *Phys. Rev. A* **2005**, *72*, 23609. [CrossRef]
49. Zhang, Y.; Jia, C.; Liang, Z. Dynamics of Two Dark Solitons in a Polariton Condensate. *Chin. Phys. Lett.* **2022**, *39*, 20501. [CrossRef]
50. Jia, C.Y.; Liang, Z.X. Dark Soliton of Polariton Condensates under Nonresonant $\mathcal{PT}$-Symmetric Pumping. *Chin. Phys. Lett.* **2020**, *37*, 40502. [CrossRef]
51. Xu, X.; Chen, L.; Zhang, Z.; Liang, Z. Dark–bright solitons in spinor polariton condensates under nonresonant pumping. *J. Phys. B* **2018**, *52*, 025303. [CrossRef]
52. Forinash, K.; Peyrard, M.; Malomed, B. Interaction of discrete breathers with impurity modes. *Phys. Rev. E* **1994**, *49*, 3400–3411. [CrossRef]
53. Astrakharchik, G.E.; Pitaevskii, L.P. Motion of a heavy impurity through a Bose-Einstein condensate. *Phys. Rev. A* **2004**, *70*, 13608. [CrossRef]